Phylogenetic positions of *Paronychomys* Jacobs and *Basirepomys* Korth and De Blieux relative to the tribe Neotomini (Rodentia, Cricetidae)

Thomas S. Kelly[1]* and Robert A. Martin[2]

[1]Research Associate, Vertebrate Paleontology Department, Natural History Museum of Los Angeles County, 900 Exposition Blvd., Los Angeles, California 90007, USA <tom@tskelly.gardnerville.nv.us>
[2]Department of Biological Sciences, Murray State University, 102 Curris Center, Murray, Kentucky 42071, USA rmartin@murraystate.edu

Abstract.—A recent study on the fossil history of North American woodrats and their relatives suggested that the Neotomini includes two subtribes: the Neotomina (woodrats; *Tsaphanomys*, *Neotoma*, *Hodomys*, *Xenomys*) and Galushamyina (reprats: *Protorepomys*, *Galushamys*, *Miotomodon*, *Repomys*, *Nelsonia*). The extinct Miocene *Lindsaymys* was proposed as a possible early neotominan, but not formally included in the Neotomini. In other studies, two extinct genera, *Basirepomys* and *Paronychomys*, occasionally have been treated as related to neotominans, but their ancestry had not been formally explored in detail. We performed a phylogenetic analysis on representatives of all genera with 40 dental and mandibular characters likely to be preserved in fossil material. The analysis resulted in a single most parsimonious tree supporting a neotominan-galushamyinan tribal classification of the Neotomini, and securely placed *Lindsaymys* within the Neotomina. None of the *Basirepomys* and *Paronychomys* species or *Protorepomys bartlettensis* nested within the Neotomini. The three *Basirepomys* species, possibly a paraphyletic group, are not closely related to *Repomys*, and *Paronychomys* (minus *P. shotwelli* = *Tsaphanomys shotwelli*) is not closely related to *Onychomys*, but is a possible sister group to the Neotomini. With the understanding that further study may remove it from *Protorepomys*, *P. bartlettensis* is tentatively retained within the genus, representing a relatively underived species possibly ancestral to both neotominan clades. *Neotoma* species of the extinct subgenus *Paraneotoma* and extant *Neotoma* may be paraphyletic at the generic level, but that determination will require further study.

Introduction

Small, relatively advanced rodents related to modern North American cricetids radiated through much of the western and central United States during the late Miocene and early Pliocene. Because they apparently did not descend from earlier, less-derived Oligocene or early Miocene North American cricetids (Martin, 1975; Lindsay, 2008), they are considered to be Asian immigrants. Originally referred to either *Copemys* Wilson, 1937, or *Peromyscus* Gloger, 1841 (Wilson, 1937; Shotwell, 1967; Lindsay, 1972), later additions and evaluations have shown late Miocene and early Pliocene cricetids to represent considerable diversity, likely including ancestors to extant North and South American cricetid clades (Jacobs, 1977; Baskin, 1979; Lindsay and Jacobs, 1984; Czaplewski, 1987; Lindsay, 2008; Korth and De Blieux, 2010; Korth, 2011; Martin and Zakrzewski, 2019; Kelly et al., 2020; Martin et al., 2020; Ronez et al., 2020).

Based on small samples of cricetid dental specimens from the late Miocene Quiburis Formation of Arizona, Jacobs (1977) erected two new genera: *Paronychomys*, with two species (*P. lemredfieldi*, which is the type species, and *P. tuttlei*) and *Galushamys*, with one species (*G. redingtonensis*). Because of a similarity in the alternation pattern of the molar cusps, Jacobs

(1977) proposed that *Paronychomys* was a cricetine cricetid related to the extant *Onychomys* Baird, 1857, but noted that *Paronychomys* differed from *Onychomys* by having more hypsodont cheek teeth and unreduced third molars. Subsequently, four additional species of *Paronychomys* were described: *P. alticuspis* Baskin, 1979; *P. woodburnei* Martin, 2008; *P. shotwelli* Korth, 2011; and *P. jacobsi* Kelly, 2013. Kelly (2013) also provisionally transferred Kellogg's (1910) *Peromyscus antiquus* to *Paronychomys* as ?*Paronychomys antiquus*. No further mention was made of a possible phylogenetic connection with *Onychomys* in any of the papers describing the latter species. Indeed, Baskin (1979, p. 706) suggested that the dentition of *Paronychomys* "...was convergent with primitive microtines and with the South American granivore *Phyllotis*," and Lindsay (2008, p. 466, fig. 27.2) regarded *Paronychomys* as closely related to *Repomys* May, 1981, and *Galushamys*.

Another mesodont cricetid, *Basirepomys*, was named by Korth and De Blieux (2010), with *Peromyscus pliocenicus* Wilson, 1937, as the type species. Korth and De Blieux (2010, p. 231) also suggested that *Basirepomys* included "...additional specimens referred to *P*. cf. *pliocenicus* elsewhere," referring to material described by Shotwell (1967) and discussed by May (1981) from the Miocene of Oregon. However, they did not formally include the Oregon material in their synonymy. Korth and De Blieux (2010) also recognized a second species, *B. robertsi*, from the Hemphillian Sevier River Formation, Utah. Korth and De Blieux (2010, p. 231) noted that *Basirepomys* molars were

CrossMark

higher crowned than those of *Peromyscus* and lower crowned than those of *Repomys*, and in the etymology section they indicated that *Basirepomys* was "…a closely related genus," to *Repomys*, but no further comparisons were made with *Repomys*. Korth (2011) later emended the diagnosis of *Basirepomys* and transferred specimens that Jacobs and Lindsay (1984) previously referred to *Peromyscus pliocenicus* from Rome, Oregon, to the new species *Basirepomys romensis* Korth, 2011. Korth (2011) also reallocated specimens from Pinole Junction, California, that May (1981) had previously referred to as *Peromyscus* cf. *pliocenicus*, to the new genus and species *Miotomodon mayi* Korth, 2011, further proposing that "*Miotomodon* is derived from *Paronychomys* rather than *Peromyscus* or *Basirepomys*" (Korth, 2011, p. 145).

In a paper proposing a phylogenetic model for the origin of cricetids related to modern woodrats, Martin and Zakrzewski (2019) established two subtribes for the Neotomini: the Neotomina (woodrats) and a redefined Galushamyina Lindsay, 2008 (common name: reprats). Neotomina included the extinct *Tsaphanomys shotwelli* (= Shotwell's [1967] *Peromyscus* cf. *pliocenicus* from Juniper Creek, Oregon = Korth's [2011] *Paronychomys shotwelli*) and extant *Neotoma* Say and Ord, 1825, *Hodomys* Merriam, 1894, and *Xenomys* Merriam, 1892 (Merriam, 1892a). The Galushamyina included the extinct *Protorepomys, Miotomodon*, *Repomys*, and *Galushamys*, plus extant *Nelsonia*. *Protorepomys* was composed of *P. mckayensis* Martin and Zakrzewski, 2019, and *P. bartlettensis* Martin and Zakrzewski, 2019, representing additional Miocene cricetid samples that Shotwell (1967) had previously referred to *Peromyscus*. At that time, Martin and Zakrzewski (2019) considered *Paronychomys lemredfieldi* to be an unusual, high-crowned relative of *Onychomys* Baird, 1857, as intended by Jacobs (1977), but transferred *Paronychomys shotwelli* to *Tsaphanomys*. They also suggested that the remaining *Basirepomys* species were neotomines unrelated to *Repomys*. This study provides a more detailed phylogenetic comparison of extinct and modern cricetids that conceivably could be related to either the woodrats or reprats, with special consideration of the problematic taxonomy of *Paronychomys* and *Basirepomys*.

Materials and methods

Dental locus designations follow standard usage with upper teeth designated by capital letters and lower teeth by lowercase letters. Dental nomenclature (Fig. 1) follows Martin et al. (2020), with modifications by Kelly et al. (2020) and this paper. Following Martin and Zakrzewski (2019, p. 1567), "enamel rings with a hollow center [on the occlusal surface] are termed 'atolls,' equal to 'fossettes,' 'islands,' or 'pits' of other authors." North American Land Mammal ages (e.g., Clarendonian, Hemphillian, and Blancan) follow Lindsay et al. (2002), Tedford et al. (2004), and Martin et al. (2008).

As noted above, some investigators have suggested that *Paronychomys* may be related to *Onychomys* (i.e., Jacobs, 1977; Martin and Zakrzewski, 2019) because they both exhibit a similar degree of alternation of the primary cusps. However, other studies have not recognized this putative relationship (e.g., Lindsay, 2008; Korth, 2011). In fact, *Onychomys* and members of Peromyscini Cockerell et al., 1914 (which are *Peromyscus*, *Habromys*

Hooper and Musser, 1964, *Megadontomys* Merriam, 1898 (Merriam, 1898 (Merriam, 1898a)), *Neotomodon* Merriam, 1898 (Merriam, 1898b), *Osgoodomys* Hooper and Musser, 1964, and *Podomys* Osgood, 1909) have very similar cusp alternation on the upper and lower molars. Lindsay (2008) allied *Paronychomys* with *Repomys* and *Galushamys* in a separate tribe (Galushamyini) from the tribe including *Onychomys*, *Peromyscus*, and *Reithrodontomys* (Democricetodontini). During our study we made extensive morphological comparisons of *Paronychomys* and *Onychomys*. There are numerous significant differences between them, indicating they are not closely related (Table 1). Moreover, genetic analyses have consistently allied *Onychomys* as the closest sister taxon to Peromyscini (e.g., Reeder and Bradley, 2004; Reeder et al., 2006; Miller and Engstrom, 2008; Keith, 2015; Steppan and Schenk, 2017).

In order to determine the phylogenetic relationships of *Paronychomys* and *Basirepomys* to Neotomini and further investigate the synapomorphies supporting the neotomine subtribes, we performed a cladistic analysis based on 40 dental and mandibular characters with representative species of each genus (Fig. 2; Table 2; our list of morphological characters and character states, and our taxon/character state matrix are provided in Appendices 1, 2). We selected the type species as representatives for extinct genera and subgenera, but during our examination we discovered a number of differences in the dental morphology of species of *Basirepomys* and *Protorepomys*. In order to determine if these differences might be phylogenetically significant, we included all species of these genera in the analysis. We also included a second species of *Paronychomys*, *P. jacobsi*, because it is much better characterized than the type species. *Copemys loxodon* (Cope, 1874) was used for the outgroup. *Copemys*, as currently recognized, is composed of a complex of nine middle to late Miocene species, probably not all congeneric (Martin and Zakrzewski, 2019; Kelly et al., 2020; Ronez et al., 2021). Most later North American Miocene Neotominae were likely derived from various members of the *Copemys* species complex (Lindsay, 2008; Martin et al., 2020; Ronez et al., 2020, 2021). Jacobs and Lindsay (1984) named a new tribe, Copemyini, for *Copemys*, which Ronez et al. (2020) considered as likely valid, but a more in-depth analysis is still needed to confirm its recognition. It should be noted that in Galushamyina and Neotomina, some character transformations occur in parallel between the earliest members through the more-derived members. These include progressive increases in lophodonty and a development of flat occlusal planes during initial to early wear. These transformations also occur in a wide variety of other rodent lineages and were not included in the analysis because of convergence.

Morphological cladistic analysis using parsimony was performed with the TNT program of the Willi Hennig Society (Goloboff and Catalano, 2016) with implicit enumeration, which guarantees the shortest (optimal) tree or trees will be found. The analysis was repeated using a standard Wagner tree search including SPR (subtree-pruning-regrafting) or TBR (tree bisection reconnection) swapping algorithms, and a new technology search with the number of trees to find with minimum length set at 1,000, all of which produced the same single most parsimonious tree as implicit enumeration. Many of the extinct cricetids in the analysis are chronologically
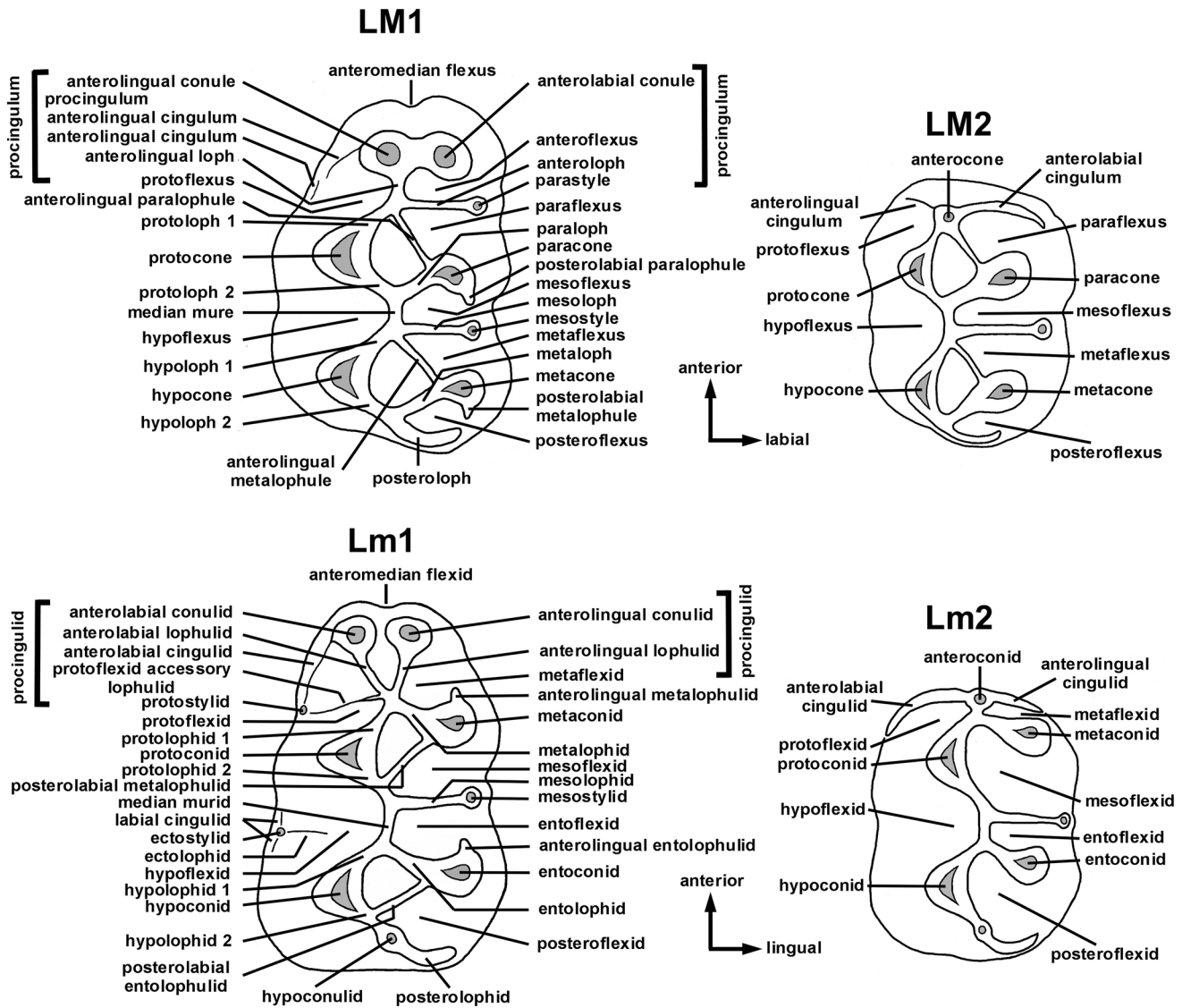
Figure 1. Dental nomenclature for cricetid teeth follows Martin et al. (2020), with modifications by Kelly et al. (2020) and this paper. The anterior structures of M2 and m2 are labeled differently because they lack a procingulum and procingulid, respectively. All terms used for M2 and m2 can be applied to M3 and m3, respectively. Not all structures are present in the taxa included in the analysis.

isolated and represented by a meager fossil record, often lacking knowledge of certain tooth positions. Thus, a relatively continuous series of temporal samples that would allow determination of qualitative or quantitative morphoclines to support any sequential ordering of character state transformations is lacking. In order to avoid any biases that might be introduced based on subjective ordering of character state transformations, all character states were treated as unordered (non-additive). Branch support was determined using bootstrap resampling (10,000 replicates with a 50% cutoff). Branch support values <50% are likely due to missing data for taxa that are poorly represented with some tooth positions unknown (Calede and Hopkins, 2012).

Abbreviations are: ap = greatest anteroposterior length; CI = consistency index; ht = height; Ma = megannum (one million years in the radioisotopic time scale); RI = retention index; tr = transverse width.

Repositories and institutional abbreviations.—AMNH FAM, American Museum of Natural History, Frick Collection, New York; IBUNAM:CNMA, Colección Nacional de Mamíferos, Departamento de Zoología, Instituto de Biología, Universidad Nacional Autónoma de México, México City; FHSM, Fort Hays Sternberg Museum, Hays; LACM, Natural History Museum of Los Angeles County, Los Angeles; LACM (CIT), California Institute of Technology specimens transferred to LACM; UALP, University of Arizona Laboratory of Paleontology, Tucson; UCMP, University of California, Museum of Paleontology, Berkeley; UCR, University of California, Riverside, transferred to UCMP (when transferred, UCR specimen numbers were modified by adding a 3 in front of the number); UMMP, University of Michigan Museum of Paleontology, Ann Arbor; UO, University of Oregon, Eugene; USNM, Smithsonian Institution National Museum of Natural History, Washington D.C.

Table 1. List of significant character differences between *Paronychomys* and *Onychomys* that indicate they are not closely related. Abbreviations: ap = greatest anteroposterior length; ht = height.

Character	*Onychomys*	*Paronychomys*
cranial		
posterior termination of nasal sutures in dorsal view	tapered posteriorly with narrow V-shape	not tapered, U-shaped
incisive foramina	terminate farther posteriorly to level of M1 procingulum	terminate more anteriorly, anterior to M1
position of anterior borders of choanae of posterior nares on palatine	positioned posteriorly, well behind posterior margins of M3s	positioned more anteriorly, at the level of posterior margins of M3s
anteromedial portion of zygomatic arch in ventral view (= origin of muscle zygomatico-mandibularis)	slopes posteriorly	more perpendicular to long axis of skull
dental		
crown height (ratio of unworn m1 protoconid ht/m1 ap)	slightly mesodont (0.53–0.54) due to tubercular increase in height	mesodont (0.60–0.65) due to coronal increase in height
occlusal planes of molars during wear	terraced in early to moderate wear	flat in early to moderate wear
M1 procingulum position relative to posterior portion of tooth	well separated, protrudes anteriorly	closer, protrudes less anteriorly
M3 occlusal pattern with wear	U-shaped	E-shaped
relative size of M3 (ratio of M3 ap/M1 ap)	significantly reduced (0.25–0.33)	slightly reduced (0.53–0.57)
m1 unworn procingulid and primary cusps	rapidly taper to sharp apices	cuspate, much less tapered with blunt apices
m1 procingulid position relative to posterior portion of tooth	protrudes well anteriorly	protrudes less anteriorly
m1 procingulid position relative to long axis of tooth	labially	centrally
m1 protoflexid and hypoflexid	wide	narrower
m1 protoflexid pocket	absent	present
m1 metaflexid	wider lingually, with procingulid and metaconid well separated, remaining open through late wear, no atoll	narrow lingually with procingulid and metaconid closely positioned lingually, closed off by early wear forming a metaflexid atoll
m3 occlusal pattern with wear	key-hole shaped	S-shaped
relative size of m3 (ratio of m3 ap/m1 ap)	significantly reduced (0.38–0.46)	slightly reduced (0.65–0.67)

Results

The cladistic analysis resulted in a single most parsimonious tree of 84 steps with a consistency index of 0.917 and a retention index of 0.972 (Fig. 3). Two distinct monophyletic branches are recognized in the analysis. The first branch includes *Lindsaymys*, *Tsaphanomys*, *Neotoma* (*Paraneotoma*) as successive sister taxa to an extant *Neotoma-Hodomys-Xenomys* clade, respectively, with the latter divided into two clades: a *Hodomys-Xenomys* clade and an extant *Neotoma* clade. The placement of the extinct subgenus *Paraneotoma* outside of the extant *Neotoma-Hodomys-Xenomys* clade suggests that the genus is not monophyletic as currently recognized. The second branch includes *Protorepomys mckayensis* and *Miotomodon* as successive sister taxa to a *Galushamys-Repomys-Nelsonia* clade, respectively, with the latter divided into two clades: a *Galushamys* clade and a *Repomys-Nelsonia* clade. *Basirepomys*, *Paronychomys*, and *Protorepomys bartlettensis* did not nest within either of the two monophyletic Neotomini clades, but are placed as successive sister taxa, respectively. The three species of *Basirepomys* do not form a monophyletic clade, but instead *B. romensis*, *B. robertsi*, and *B. pliocenicus* are placed as successive sister taxa to *Paronychomys*, respectively. The two species of *Protorepomys* also do not form a monophyletic clade.

Discussion

The analysis recognized the following seven ancestral synapomorphies for all ingroup taxa relative to *Copemys*: (1) M1 anteroloph absent; (2) M2 mesoloph short and labially directed; (3) m1 procingulid centrally positioned; (4) m1 metaconid and procingulid closely positioned lingually and fused, with wear forming a metaflexid atoll; (5) m1 protoflexid extends to base of protoconid and is unpocketed; (6) m3 mesolophid absent; and (7) mesodont to hypsodont due to coronal increase in crown height (Fig. 3, node 1). Of these, numbers 4 and 7 also distinguish all ingroup taxa in the analysis from members of Neotominae Merriam, 1894, and tribes Baiomyini Musser and Carleton, 2005, Reithrodontomyini Vorontsov, 1959, and Peromyscini Cockerell et al., 1914.
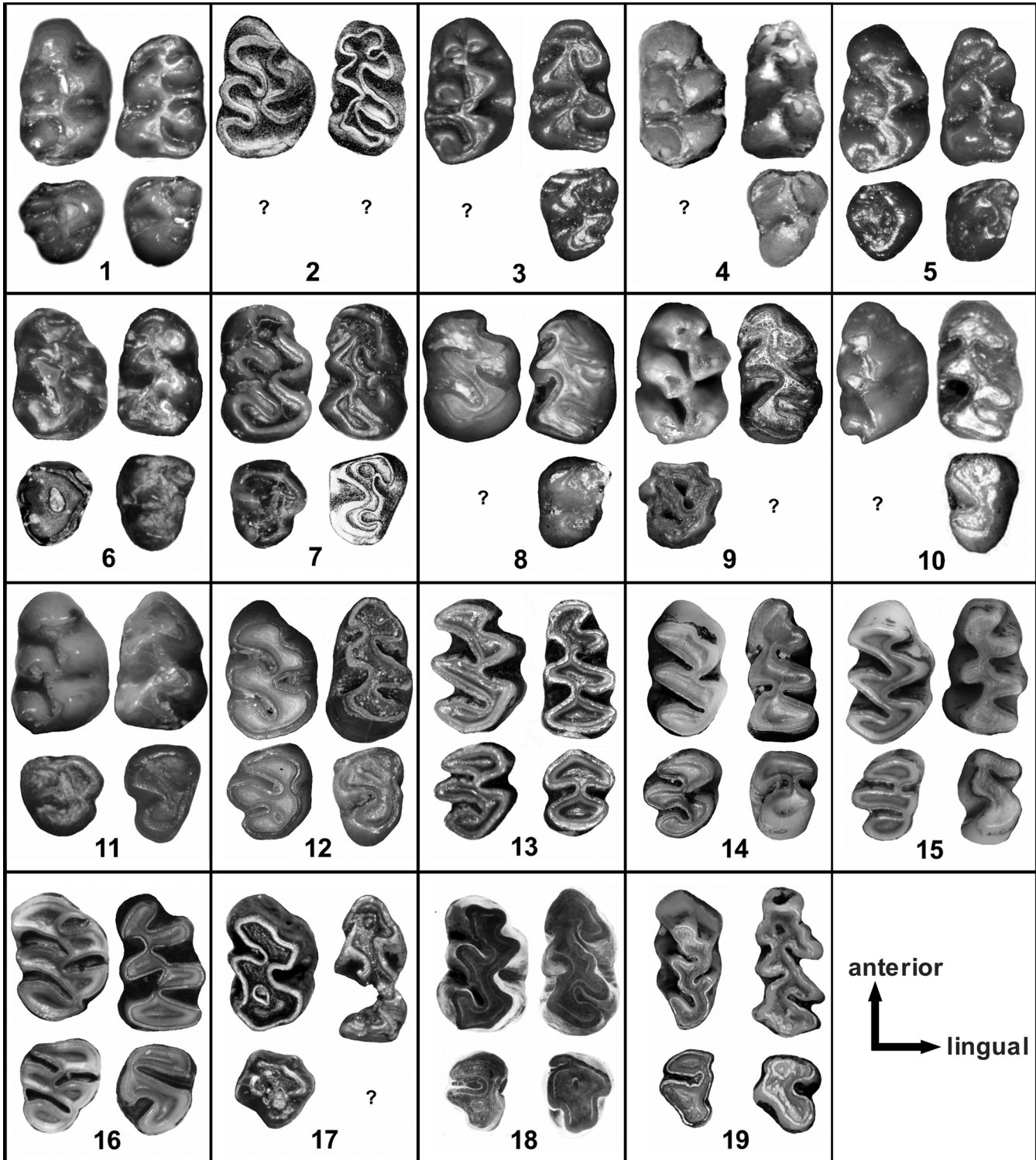
←

Figure 2. M1 (upper left in each quadruplet), M3 (lower left), m1 (upper right), and m3 (lower right) of species in cladistic analyses. Question mark indicates tooth position unknown. All occlusal views. (**1**) *Copemys loxodon*, LM1 (UCMP 317394, reversed), LM3 (UCMP 317400, reversed), Lm1 (UCMP 317625, reversed), Rm3 (UCMP 317546, reversed), photos by C. Ronez; (**2**) *Basirepomys pliocenicus*[1], RM1 (LACM [CIT] 1968), Rm1 (LACM [CIT] 1966, holotype), from Wilson (1937); (**3**) *Basirepomys romensis*, LM1 (USNM 23564, reversed), Rm1, (USNM 23567, reversed), Lm3 (UMNH 23566), photos of E. Lindsay casts; (**4**) *Basirepomys robertsi*[2], LM1 (UMNH VP 18749, reversed), Rm1 (UMNH VP 18751, holotype, reversed), Rm3 (UMNH VP 18752), from Korth and De Blieux (2010); (**5**) *Paronychomys lemredfieldi*, RM1 and RM3 (AMNH FAM 3249), Rm1 and Rm3 (AMNH FAM 3430, reversed), photos of E. Lindsay casts; (**6**) *Paronychomys jacobsi*, RM1 (LACM 156279), LM3 (LACM 156277, reversed), Lm1 (LACM 156289), Lm3 (LACM 156287), photos by T. Kelly; (**7**) *Protorepomys bartlettensis*, LM1 (UO 24957, reversed), LM3 (UO 25078, reversed), Lm1 (UO 25591); photos by K. Tate-Jones, Lm3 (UO 21720); from Shotwell (1967); (**8**) *Protorepomys mckayensis*, RM1 (UO 26942), Lm1 (UO 24603), Rm3 (UO 21720), photos by K. Tate-Jones; (**9**) *Miotomodon mayi*[2], LM1 (UCMP 82669, reversed), LM3 (UCMP 83672, reversed), Lm1 (UCMP 82671), from Korth (2011); (**10**) *Tsaphanomys shotwelli*, LM1 (UO 21716, reversed), photo by K. Tate-Jones; Lm1 (UO 21719), Lm3 (UO 21270), from Korth[2] (2011); (**11**) *Lindsaymys takeuchii* Kelly and Whistler, 2014, RM1 (LACM 126050, holotype), RM3 (LACM 156397), Rm1 (LACM 156394, reversed), Lm3 (LACM 156521), photos by T. Kelly; (**12**) *Neotoma* (*Paraneotoma*) *quadriplicata* Hibbard, 1941, LM1 (UMMP 41198, reversed); photo by A. Rountrey; LM3 (UMMP 41196, reversed), Rm1 (FHSM 14330, reversed), Rm3 (UMMP 41196), photos by R. Zakrzewski; (**13**) *Neotoma cinerea occidentalis* Baird, 1855, RM1 and RM3 (MVZ 69441), Lm1 and Lm3 (MVZ 69441), photos by Jessica Blois, UC Merced; (**14**) *Neotoma lepida lepida*[3], LM1 and LM3 (MVZ 10438, reversed), Rm1 and Rm3 (MVZ 10438, reversed), photos by C. Conroy; (**15**) *Hodomys alleni*, LM1 and LM3 (IBUNAM:CNMA 8912, reversed), from Silva and Cuenca (2020a), Rm1 and Rm3 (IBUNAM:CNMA 46970, reversed), from Cervantes et al. (2016a); (**16**) *Xenomys nelsoni* Merriam, 1898 (Merriam, 1898a), LM1 and LM3 (IBUNAM:CNMA 5829, reversed), from Silva and Cuenca (2020b); Rm1 and Rm3 (IBUNAM:CNMA 42968, reversed), from Cervantes et al. (2016b); (**17**) *Galushamys redingtonensis*, RM1 (UALP 6013), RM3 (UALP 6020), Rm1 (UALP 6013, reversed), photos by T. Kelly; (**18**) *Repomys gustelyi*[2] May, 1981, LM1 (UCR 20147= UCMP 320147, reversed), RM3 (UCR 20156 = UCMP 320156), Lm1 (UCR 20158 = UCMP 320158), Rm3 (UCR 20178 =UCMP 320178, reversed), from May (1981); (**19**) *Nelsonia goldmani* Merriam, 1903, RM1 (USNM 125816), LM3 (USNM 90893, reversed), Lm1 (USNM 125816), Lm3 (USNM 125602), photos by C. Ronez. [1]With permission of the Carnegie Institution for Science; [2]with permission from Taylor & Francis; [3]with permission of the Museum of Vertebrate Zoology Archives, University of California, Berkeley. Not to scale, all specimens adjusted to equal size for comparison.

Based on 10 dental characters, Martin and Zakrzewski's (2019) cladistic analysis recognized two subtribes within the tribe Neotomini: the Galushamyina and Neotomina. Galushamyina was restricted to *Tsaphanomys, Neotoma, Hodomys,* and *Xenomys*, whereas Neotomina was restricted to *Protorepomys, Miotomodon, Galushamys, Repomys,* and *Nelsonia*. They also suggested that *Lindsaymys* might represent a basal neotominan, but their limited cladistic analysis did not support this allocation and instead placed *Lindsaymys* as the closest sister taxon to Galushamyina plus Neotomini.

Our cladistic analysis with 40 characters robustly supports the monophyletic statuses and original compositions of the Galushamyina and Neotomina, except for *P. bartlettensis* (see below) and the addition of *Lindsaymys* as a basal neotominan. The latter is supported by the shared ancestral synapomorphy of the absence of an M3 protoflexus. Ancestral synapomorphies recognized for the Neotomini are enlargement of M3 talon, being only slightly smaller than the trigon (secondarily reduced in galushamyinans), and the absence of an m3 posteroflexid

(Fig. 3, node 7). A previously unrecognized synapomorphy for extant Neotomini is the relative position of the choanae of the posterior nares to the tooth row, wherein the anteriormost borders of the choanae extend anteriorly well forward of the posterior margins of the M3s (Fig. 4). The pleisomorphic state for this character appears to be one in which the anterior margins of the choanae are even with the M3 posterior margins, as seen in Oligocene cricetids and one extinct species in our analysis, *P. jacobsi*. This character is only known for one species of *Copemys, C. russelli* James, 1963, which also has the pleisomorphic state. In the Neotominae subtribes Baiomyini, Reithrodontomyini, and Peromyscini, the anteriormost borders of the choanae are even to well posterior of the posterior margins of the M3s. In Ochrotomyini Musser and Carleton, 2005, they are slightly anterior of the posterior margins of the M3s, but less so than extant Neotomini. This character was not included in the cladistic analysis because its state is undetermined for most of the extinct taxa.

A common ancestral node uniting the three species of *Basirepomys* was not recognized in the analysis; instead the species are placed as successive sister taxa of successive common ancestors to *Paronychomys, Protorepomys bartlettensis* plus Galushamyina and Neotomina. Although *B. romensis* possesses several pleisomorphic states relative to *B. robertsi* and *B. pliocenicus*, the following apomorphies were recognized: (1) a strongly bilobed M1 procingulum, and (2) a slightly bilobed m1 procingulid during very early wear. *Basirepomys robertsi* is more derived than *B. romensis* by having the following ancestral synapomorphies also shared with the common ancestor of *B. pliocenicus* plus all remaining taxa analyzed: (1) an M1 parastyle absent, and (2) an m1 mesolophid absent (Fig. 2, node 2). *Basirepomys pliocenicus* is more derived than *B. robertsi* in the following ancestral synapomorphies also shared with the common ancestor of *Paronychomys* plus all remaining taxa analyzed: (1) M1 mesolophid absent, (2) M1 mesostyle absent, and (3) M2 mesoloph absent (Fig. 2, node 3). Our analysis does not support any species of *Basirepomys* as closely related to *Repomys* or any other member of Galushamyina. The acquisition of successive derived character states in the species of *Basirepomys* suggests that

Table 2. Representative species of genera included in cladistic analysis (†, extinct).

| Taxon/author |
| --- |
| †*Copemys loxodon* (Cope, 1874)—type species (outgroup) |
| †*Basirepomys pliocenicus* (Wilson, 1937)—type species |
| †*Basirepomys robertsi* Korth and De Blieux, 2010 |
| †*Basirepomys romensis* Korth, 2011 |
| †*Galushamys redingtonensis* Jacobs, 1977—type species |
| *Hodomys alleni* (Merriam, 1892) (Merriam, 1892b)—type species |
| †*Lindsaymys takeuchii* Kelly and Whistler, 2014—type species |
| †*Paronychomys lemredfieldi* Jacobs, 1977—type species |
| †*Paronychomys jacobsi* Kelly, 2013 |
| †*Protorepomys bartlettensis* Martin and Zakrewski, 2019 |
| †*Protorepomys mckayensis* Martin and Zakrewski, 2019—type species |
| †*Miotomodon mayi* Korth, 2011—type species |
| *Nelsonia goldmani*—(Merriam, 1897) |
| *Neotoma* (†*Paraneotoma*) *quadriplicata* Hibbard, 1941—type species of subgenus Hibbard 1967 |
| *Neotoma cinerea* (Ord, 1815) |
| *Neotoma lepida* Thomas, 1893 |
| †*Tsaphanomys shotwelli* (Korth, 2011)—type species by designation Martin and Zakrewski, 2019 |
| †*Repomys gustelyi* May, 1981—type species |
| *Xenomys nelsoni* Merriam, 1892 (Merriam, 1892a) |
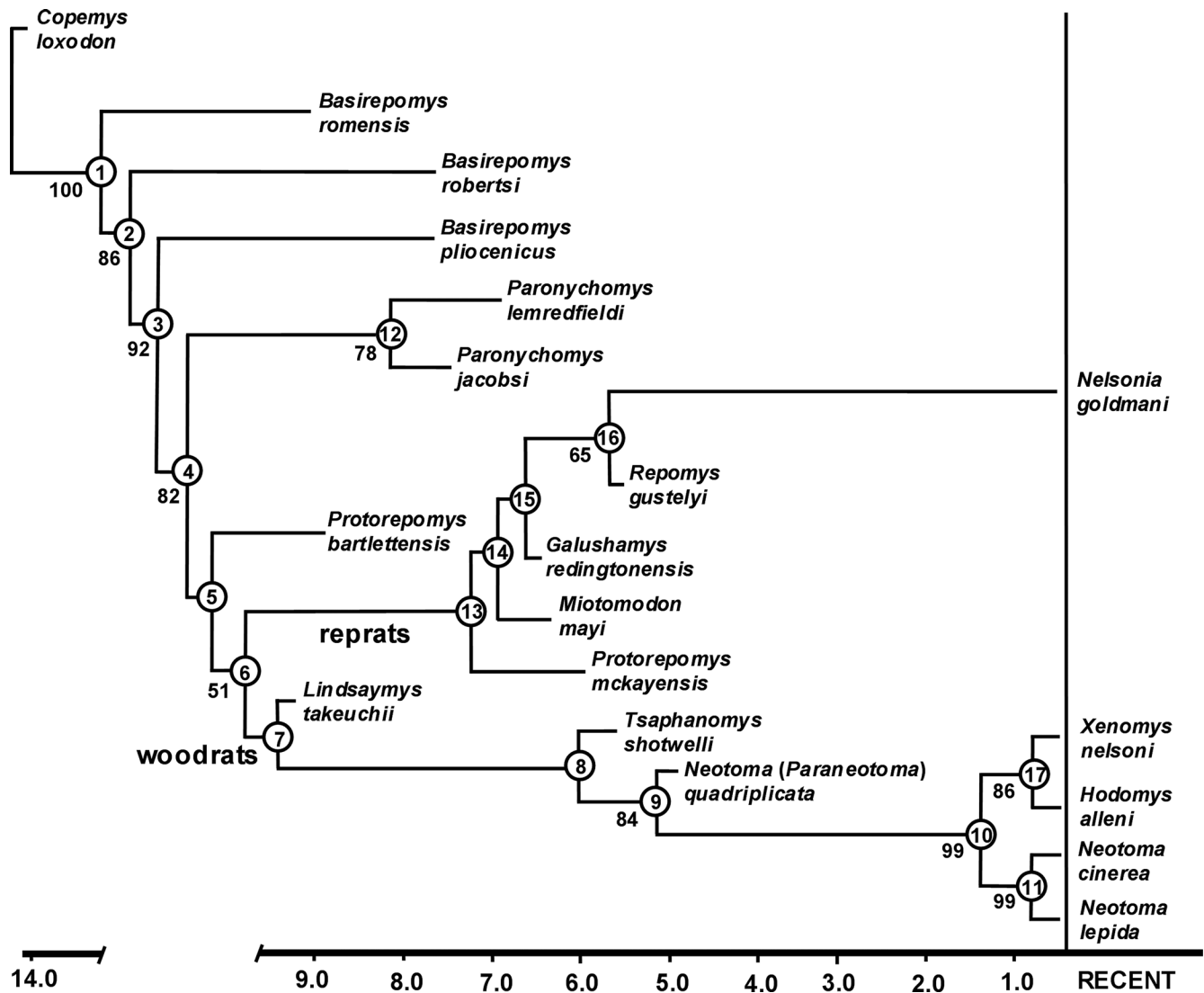
Figure 3. Single most parsimonious tree of 84 steps, CI = 0.917, RI = 0.972, using implicit enumeration. Values below branches are bootstrap support when >50%. The cladogram is supported by the following list of hypothesized ancestral synapomorphies (number to left of period denotes character number and number to right of period denotes character state). Node 1—1.2, 11.1, 17.1, 22.1, 26.2, 30.1, 33.1. Node 2—2.1, 18.4. Node 3—3.4, 4.1, 11.4. Node 4—5.1, 26.1. Node 5—34.1. Node 6 —16.1, 36.1. Node 7—13.2. Node 8—26.3. Node 9—28.1, 37.1. Node 10—22.2, 23.2, 24.1, 26.5, 30.3, 34.3. Node 11—9.1, 29.1, 32.3, 35.1, 39.1. Node 12—8.1, 10.1, 13.2, 15.3, 25.1, 27.1, 30.2. Node 13—11.2, 18.3, 26.4. Node 14—3.2. Node 15—13.1, 14.1, 15.2, 16.2. Node 16—12.2. Node 17—38.3, 39.1, 40.1. Apomorphies for terminal taxa are: *Basirepomys romensis* 6.1, 21.1; *Basirepomys robertsi* 21.3; *Basirepomys pliocenicus* 21.2; *Paronychomys lemredfieldi* 21.1; *Protorepomys bartlettensis* 1.1, 3.1, 18.1, 23.1; *Miotomodon mayi* 26.3; *Galushamys redingtonensis* 3.3, 7.1, 11.3; *Nelsonia goldmani* 13.2; *Neotoma lepida* 7.2, 26.6; *Neotoma cinerea* 20.1.

the genus as currently recognized is paraphyletic and should be evaluated further.

Paronychomys is placed as the closest sister taxon to *P. bartlettensis* plus Galushamyina and Neotomina (Fig. 2, node 4). The monophyly of *Paronychomys* is well supported by the following synapomorphies (Fig. 3, node 12): (1) well-developed, shelf-like M1–2 labial flexi and hypoflexus; (2) well-developed, shelf-like m1–2 lingual flexids and hypoflexid; (3) M3 hypoflexus absent to vestigial; (4) M3 hypocone weakly developed; and (5) m1 procingulid anterolabial cingulid well developed, extending posteriorly and connecting to base of protoconid, forming a distinct pocketed protoflexid. May (1981) and Korth (2011) proposed that *Repomys* may have been derived from *Miotomodon*. In our analysis, *Miotomodon* is placed as the closest sister taxon to a *Galushamys-Repomys-Nelsonia* clade,

supported by two ancestral synapomorphies (Fig. 2, node 14): (1) M2 mesolophid significantly reduced to a mesolophule; and (2) a shallow m1 metaflexid, with the metaconid and procingulid connected during initial wear. Korth (2011) also proposed that *Miotomodon* was derived from *Paronychomys* rather than *Basirepomys*, which our analysis does not support.

Kellogg (1910) named *Peromyscus antiquus* based on a partial dentary with m1–3 from the early Hemphillian Thousand Creek Beds of northern Nevada (Fig. 5), and Wilson (1937) referred a partial dentary with m1–3 (LACM[CIT] 1812) to the species from the early Hemphillian Coal Valley Formation of Smith Valley, Nevada. Wilson (1937) and Hoffmeister (1945) noted that *P. antiquus* may represent a genus distinct from *Peromyscus* because of its larger size and higher crowned teeth. *Peromyscus antiquus* is at least 1.5 Ma older or more than
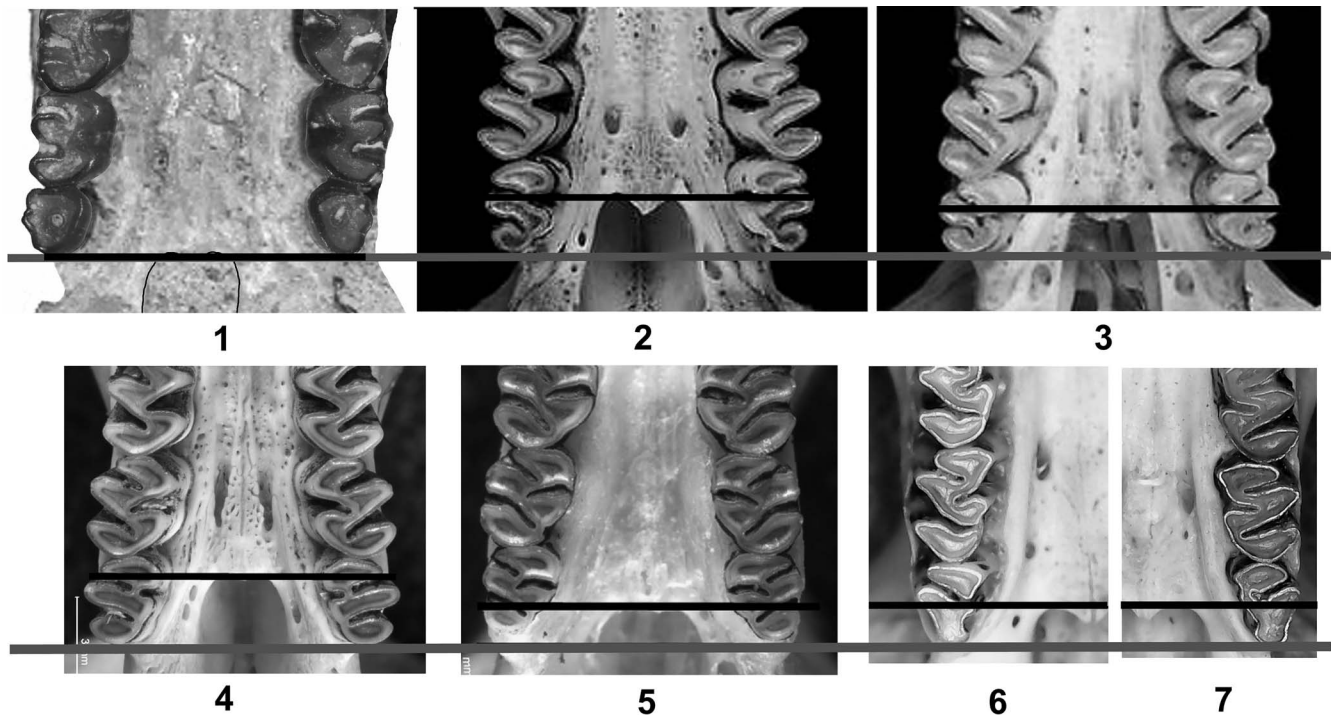
Figure 4. Ventral views of posterior palates showing synapomorphic character state of anterior position of anteriormost choanae borders of posterior nares (thick black lines) relative to posterior margins of M3s (thick gray lines) in representatives of extant Neotomini versus pleisomorphic state seen in *Paronychomys*, *Copemys russelli*, and primitive Oligocene cricetids where anteriormost choanae borders are even with posterior borders of M3s. (**1**) *Paronychomys jacobsi*[1], LACM 156274 (holotype, choanae anterior borders outlined by thin black lines because posterior nares filled with rock matrix; thick black line overlaps thick gray line with both equal in position); (**2**) *Neotoma cinerea occidentaltis*[2] (MVZ 11152); (**3**) *Neotoma lepida lepida*[3] (MVZ 10438); (**4**) *Hodomys alleni elatturus*[4] Osgood, 1938 (IBUNAM: CNMA 8912); (**5**) *Xenomys nelsoni*[5], (IBUNAM:CNMA 5829); (**6, 7**) *Nelsonia goldmani*[6] (USNM 91965 and USNM 90893, respectively). [1]Photo by T. Kelly; [2]photo by J. Blois; [3]with the permission of The Museum of Vertebrate Zoology Archives, University of California, Berkeley; [4, 5]from Silva and Cuenca (2020a, 2020b); [6]photos by C. Ronez. Not to scale, all adjusted to equal M1–3 lengths.

the oldest species of *Paronychomys* sensu stricto, *P. jacobsi* (Kelly, 2013). Kelly (2013) provided a detailed comparison of *P. antiquus* to *Paronychomys* and proposed that it was likely ancestral to later species of *Paronychomys* and questionably referred it to the genus as ?*Paronychomys antiquus*. It exhibits the following shared characters with other *Paronychomys* species (Kelly, 2013; this paper): (1) mesodont; (2) m1–2 primary cusps alternate and slant slightly inwards towards the centerlines of the teeth; (3) m1 procingulid subcircular and centrally positioned; (4) m1 metaconid positioned close lingually to the procingulid, which would form a shallow metaflexid atoll with further wear; (5) m1 protoflexid pocketed; (6) m1–3 accessory molar stylids and lophids absent; (7) well-developed and shelf-like labial and lingual cingulids; (8) relatively long, procumbent diastema; (9) ascending ramus rises between m2–3; and (10) masseteric scar relatively narrow, terminating anteriorly below m1 protoconid. It differs from later species of *Paronychomys* by the following (Kelly, 2013; this paper): (1) slightly lower crowned (mean ratio of m1 protoconid ht/ap = 0.49, versus mean range for other species = 0.53–0.65); (2) m2–3 anterior cingulids better developed; (3) m1–3 occlusal surfaces with slightly less tendency to form flat occlusal planes in early wear; (4) m1 metaconid and procingulid joined lingually at slightly later wear stage; (5) m3 entoconid slightly less developed; and (6) m3 slightly less reduced relative to m2 (ratio of m3 ap/m2 ap = 0.89, versus mean range for other species = 0.77–0.82). These differences indicate that later species of

Paronychomys are more derived. We did not include *P. antiquus* in the analysis because so many of its character states are unknown. However based on the above shared character states, we provisionally assign *P. antiquus* to *Paronychomys* sensu lato, recognizing that additional specimens, including upper molars, are needed to confirm this assignment.

A common ancestral node uniting the two species of *Protorepomys* was not recognized in the analysis; instead *P. bartlettensis* is placed as the closest sister taxon to Neotomini and *P. mckayensis* is recognized as a basal galushamyinan and the sister taxon to all other galushamyinans (Fig. 3, nodes 5, 13). *Protorepomys mckayensis* is more derived than *P. bartlettensis* by the following: (1) M1 anteroloph absent; (2) M1 mesoloph absent; (3) m1 metaflexid very shallow, lacking an atoll between the procingulum and metaconid; (4) m1 mesolophid reduced to a mesolophulid; and (5) m3 posteroflexid absent. *Protorepomys bartlettensis* also possesses the following apomorphies: (1) M1 anteroloph fused labially to procingulum forming an atoll; (2) extremely deep m1 protoflexid extending to near the lingual enamel margin between the metaconid and procingulid forming a shallow atoll at its termination; and (3) very well-developed, long m1 procingulid anterolabial cingulid. The position of *P. bartlettensis* relative to that of *P. mckayensis* in the analysis implies that *Protorepomys* is paraphyletic. Even though *P. bartlettensis* possesses a number of pleisomorphic states relative to galushamyinans and neotominans as recognized in the analysis, several characters appear transitional. The m1 mesolophid is
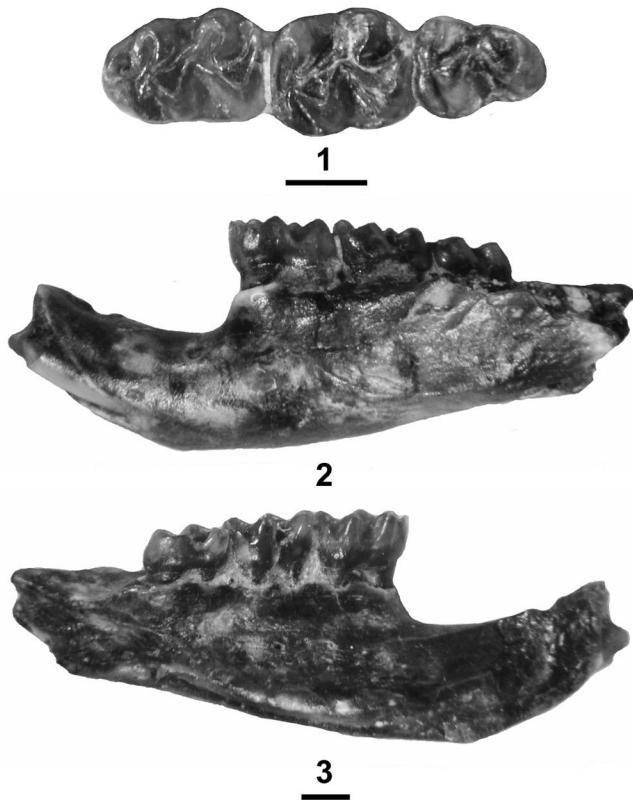
Figure 5. *Paronychomys antiquus*, holotype left dentary with m1–3 (UCMP 12571): (**1**) occlusal view; (**2**) labial view; (**3**) lingual view. Scale bars for (**1**) and (**2, 3**) 1 mm. Photos by P. Holroyd, UCMP.

distinct, but reduced, slightly anterolingually directed and somewhat fused to the entolophid. This appears transitional between the pleisomorphic state of a more labially directed mesolophid with its origin clearly from the protolophid 2 and the mesolophulid seen in galushamyinans. The molars of *P. bartlettensis* wear relatively flat after moderate wear and exhibit some lophodonty, which also is seen in *P. mckayensis*. *Protorepomys bartlettensis* is ca. 3 Ma older than *P. mckayensis* (Shotwell, 1967; McClellan and Smith, 2020), so it is not surprising that it possesses a number of pleisomorphic characters. Despite our analysis, the possibility that *P. mckayensis* was derived from *P. bartlettensis* or an unknown species closely related to it cannot be ruled out. Unfortunately further comparisons are difficult because both species are known from a very limited number of teeth, with some tooth positions unknown for each species. Although *P. bartlettensis* possesses a number of characters that differ from *P. mckayensis* and our analysis suggests that *Protorepomys* is paraphyletic, until additional more-complete material is available for further study to confirm this, we tentatively retain it in *Protorepomys*.

Protorepomys mckayensis plus all other galushamyinans (Galushamyina) are united by the following the ancestral synapomorphies (Fig. 3, node 13): (1) M2 mesolophule present; (2) m1 mesolophulid present; and (3) a shallow m1 metaflexid, with the metaconid and procingulid connected at initial wear. *Miotomodon* is recognized as the closest sister taxon of a *Repomys-Nelsonia* clade plus *Galushamys*, united by the ancestral synapomorphy of an M1 mesolophule present (Fig 3, node

14). *Galushamys* and the *Repomys-Nelsonia* clade are united by the following ancestral synapomorphies (Fig. 3, node 15): (1) a shallow M3 protoflexus; (2) a shallow, weakly developed M3 hypoflexus; (3) a weakly developed M3 hypocone; and (4) M3 talon significantly reduced relative to trigon (talon tr/trigon tr ratio ≤0.50).

Galushamys is distinguished from other galushamyinans by having the following autapomorphies: (1) the M1–2 mesoloph is significantly reduced, fused anteromedially to the paraloph and connected to the metacone by early wear, resulting in an atoll between the paracone; and metacone; and (2) the M1 protoflexus is usually very shallow and slightly provergent.

The *Nelsonia-Repomys* clade is supported by a single synapomorphy (Fig.3, node 16): the M3 occlusal outline wears to a distinctive F-shaped pattern due to a deep paraflexus and reduced metaflexus that commonly forms an atoll at initial to very early wear (Fig. 2). When considering only extant species, our analysis placed *Nelsonia* as the closest sister taxon to a *Neotoma-Hodomys-Xenomys* clade. This relationship also has been recognized in recent molecular studies (e.g., Steppan and Schenck, 2017; León-Tapia and Cervantes, 2021).

Martin and Zakrzewski (2019) concluded that the extinct *Neotoma* (*Paraneotoma*) and extant *Neotoma* formed a clade that was the sister clade to a *Hodomys-Xenomys* clade. However no hypothesized ancestral synapomorphies were identified in support of the common ancestors of either of these clades. Our analysis places *Neotoma* (*Paraneotoma*) as the closest sister clade to an extant *Neotoma* clade plus a *Hodomys-Xenomys* clade. This is supported by the following ancestral synapomorphies shared by extant *Neotoma*, *Hodomys* and *Xenomys* (Fig. 3, node 10) and lacking in *Neotoma* (*Paraneotoma*): (1) m1 procingulid labially positioned; (2) m1 protoflexid nearly perpendicular to long axis of tooth; (3) m1 entoflexid deep and nearly perpendicular to long axis of tooth; (4) m1 metaflexid deep and wide, with the metaconid and procingulid well separated throughout wear; (5) m1 procingulid anterolabial cingulid weakly developed and widely separated from protoconid; and (6) m3 entoflexid deep, relatively straight, and widely open lingually through wear never forming an atoll. These synapomorphies imply that extant *Neotoma*, *Hodomys*, and *Xenomys* share a common ancestor that split off from that of their common ancestor with *Neotoma* (*Paraneotoma*). This further implies that if *Neotoma* (*Paraneotoma*) and extant *Neotoma* are included in the same genus, *Neotoma* becomes paraphyletic. Hibbard (1967, p. 130) proposed that *Neotoma* (*Paraneotoma*) "…is closely related to or is the stock that gave rise to *Neotoma* [= *Hodomys*] *alleni* [Merriam, 1892] [Merriam, 1892b]." Here we tentatively retain *Paraneotoma* as a subgenus of *Neotoma*, but recognize that if future detailed analyses support this phylogenetic scenario, *Paraneotoma* would deserve elevation to generic rank.

The *Xenomys-Hodomys* clade is supported by the following ancestral synapomorphies: (1) a reduced, small mental foramen; (2) a reduced incisor capsular process; and (3) the masseteric scar is positioned low on the horizontal ramus (Fig. 3, node 17). Although not included in the analysis because the character states for extinct species are unknown, an additional soft-tissue character allying *Xenomys* and *Hodomys* is the morphology of the glans penis (Hooper, 1960; Genoways and Birney, 1974; Carleton, 1980). They both share the following characters

(Hooper, 1960, pl. 8): (1) relatively short, length/width ratio = 1.3–1.9; (2) mid-dorsal and mid-ventral troughs; (3) two urethral processes and dorsal papillae present; and (4) terminal crater nearly filled, with a bulbous mass covering tip of baculum that is free of the crater. *Neotoma cinerea* Ord, 1815, and *N. lepida* Thomas, 1893, differ from *Xenomys* and *Hodomys* by the following (Hooper, 1960, pls. 6, 7): (1) greater length/width ratio (4.5–9.2); (2) simpler form (lack bulbous mass); (3), single, undivided urethral process; and (4) troughs lacking. Although the glans penis of certain other extant *Neotoma* are relatively short with length/width ratios varying from 1.26–2.2 (e.g., *N. albigula* Hartley, 1894), all lack troughs and the bulbous mass in the terminal crater (Hooper, 1960).

Further supporting evidence that *Xenomys* and *Hodomys* are closely related to extant *Neotoma* include molecular analyses that place *Xenomys* and *Hodomys* as either the closest successive sister taxa to extant *Neotoma*, respectively (Reeder and Bradley, 2004; Matocq et al., 2007) or within a *Hodomys-Xenomys* clade that is the closest sister clade to extant *Neotoma* (Steppan and Schenk, 2017; León-Tapia and Cervantes, 2021).

Conclusions

The division of the Neotomini subtribes, Galushamyina (reprats) and Neotomina (woodrats), is well supported by our analysis. Galushamyina is comprised of *Protorepomys mckayensis*, *Miotomodon*, *Galushamys*, *Repomys*, and extant *Nelsonia*. Neotomina is composed of *Lindsaymys*, *Neotoma* (*Paraneotoma*), *Hodomys*, *Xenomys*, and extant *Neotoma*. An additional synapomorphy uniting extant Neotomini is the anterior position of the choanae of the posterior nares relative to the posterior margins of the M3s. *Neotoma* (*Paraneotoma*) is the closest sister taxon to an extant *Neotoma-Hodomys-Xenomys* clade, the latter divided into an extant *Neotoma* clade and a *Hodomys-Xenomys* clade. This suggests that *Neotoma* (*Paraneotoma*) and extant *Neotoma* are paraphyletic at the generic level, but further study will be necessary to make this determination. An additional synapomorphy uniting *Hodomys* and *Xenomys*, not included in the analysis because it is unknown for extinct taxa, is the distinctive suite of shared characters seen in the glans penis.

Paronychomys shares with Neotomini a closely positioned m1 metaconid and procingulid, fused either initially or during early wear, a progressive coronal increase in molar crown height, and a tendency to form a flat occlusal plane during early wear, suggesting that *Paronychomys* is the sister taxon to *Protorepomys bartlettensis* plus Neotomini. Although *Basirepomys* may be paraphyletic, all three species exhibit a closely positioned m1 metaconid and procingulid, but these structures do not fuse until very late wear, indicating that they are less derived than the condition seen in *Paronychomys*, *P. bartlettensis*, and Neotomini. Species of *Basirepomys* also exhibit a number of other pleisomorphic characters relative to *Paronychomys*, *P. bartlettensis*, and Neotomini, further indicating they are more removed from Neotomini than *Paronychomys*. Whether the three species of *Basirepomys* represent a side branch of successive sister taxa of Neotominae or the successive sister taxa to *Paronychomys*, *P. bartlettensis*, and Neotomini is uncertain at this point, but none of them is closely related to *Repomys* or

other Galushamyina. If the paraphyly of *Basirepomys* as recognized in our analysis is confirmed by additional studies, then establishing two new generic ranks for *B. romensis* and *B. robertsi* to separate them from the type species, *B. pliocenicus*, would be warranted.

Protorepomys mckayensis nests within Galushamyina as a basal galushamyinan, but *P. bartlettensis* exhibits a number of pleisomorphic characters that suggest the genus is paraphyletic, with *P. bartlettensis* as the possible closest sister taxon to Neotomini. However, because *P. bartlettensis* is currently represented by only five isolated teeth representing three tooth positions (Shotwell, 1967; Martin and Zakrzewski, 2019), erecting a new genus is unjustified at this time. However, if the discovery of additional material and further study confirms this paraphyly, erecting a new genus for *P. bartlettensis* would be warranted.

Acknowledgments

References

Baird, S.F., 1855, Characteristics of some new species of North American Mammalia, collected chiefly in connections with the United States surveys of a railroad route to the Pacific: Proceedings of the Academy of Natural Sciences, Philadelphia v. 7, p. 333–336.

Baird, S.F., 1857, Mammals of North America; the descriptions of species based chiefly on the collections in the Museum of the Smithsonian Institution: Philadelphia, J.H. Lippincott & Co., 752 p.

Baskin, J.A., 1979, Small mammals of the Hemphillian age White Cone Local Fauna, northeastern Arizona: Journal of Paleontology, v. 53, p. 695–708.

Calede, J.J.M., and Hopkins, S.B., 2012, New material of *Alphagaulus pristinus* (Mammalia, Rodentia, Mylagaulidae) from the Deep River Formation (Montana, U.S.A.): implications for ecology, ontogeny, and phylogeny: Journal of Vertebrate Paleontology, v. 32, p. 151–165.

Carleton, M.D., 1980, Phylogenetic relationships in neotomine-peromyscine rodents (Muroidea) and a reappraisal of the dichotomy within New World Cricetinae: Miscellaneous Publications of the Museum of Zoology, University of Michigan, v. 157, p. 1–146.

Cervantes, F.A., Castañón, C.E., Sánchez, Vargas, J., and Hortelano, Y., 2016a, Molares de la mandíbula inferior derecha de la rata arborícola *Hodomys alleni*: http://unibio.unam.mx/irekani/bitstream/123456789/37951/1/11894.jpg. [Jan 2021]

Cervantes, F.A., Castañón, C.E., Sánchez, Vargas, J., and Hortelano, Y., 2016b. Molares de la mandíbula inferior derecha de la rata de Magdalena *Xenomys nelsoni*. http://unibio.unam.mx/irekani/handle/123456789/37950?proyecto=Irekani. [Jan 2021]

Cockerell, T.D.A., Miller, L.I., and Printz, M., 1914, The auditory ossicles of American rodents: Bulletin of the American Museum of Natural History, v. 33, p. 347–380.

Cope, E.D., 1874, Notes on the Santa Fé Marls, and some of the contained vertebrate fossils: Proceedings of the Academy of Natural Sciences of Philadelphia, v. 26, p. 147–152.

Czaplewski, N.J., 1987, Sigmodont rodents (Mammalia: Muroidea; Sigmodontinae) from the Pliocene (early Blancan) of the Verde Formation, Arizona: Journal of Vertebrate Paleontology, v. 7, p. 183–199.

Genoways, H.H., and Birney, E.C., 1974, *Neotoma alleni*: Mammalian Species, v. 41, p. 1–4.

Gloger, C.W.L., 1841, Gemeinnǔbiges Hand- und Bilfsbuch der Naturgefchichte: Breslau, Berlag von Aug Schultz and Company, 495 p.

Goloboff, P.A., and Catalano, S.A., 2016, TNT version 1.5, including a full implementation of phylogenetic morphometrics: Cladistics, v. 32, p. 221–238.

Hartley, F., 1894, Description of a new species of woodrat from Arizona: Proceedings of the California Academy of Science, ser. 2, v. 4, p. 157–160.

Hibbard, C.W., 1941, New mammals from the Rexroad Fauna, upper Pliocene of Kansas: American Midland Naturalist, v. 26, p. 337–368.

Hibbard, C.W., 1967, New rodents from the late Cenozoic of Kansas: Papers of the Michigan Academy of Science, Arts, and Letters, v. 52, p. 115–132.

Hoffmeister, D.F., 1945, Cricetine rodents of the middle Pliocene of the Mulholland Fauna, California: Journal of Mammalogy, v. 26, p. 186–191.

Hooper, E.T., 1960, The glans penis in *Neotoma* (Rodentia) and allied genera: Occasional Papers of the Museum of Zoology, University of Michigan, v. 618, p. 1–20.

Hooper, E.T., and Musser, G.G., 1964. Notes on classification of the rodent genus *Peromyscus*: Occasional Papers, Museum of Zoology, University of Michigan, v. 635, p. 1–13.

Jacobs, L.L., 1977, Rodents of the Hemphillian age Redington Local Fauna, San Pedro Valley, Arizona: Journal of Paleontology, v. 51, p. 505–519.

Jacobs, L.L., and Lindsay, E.H., 1984, Holarctic radiation of Neogene muroid rodents and the origin of South American cricetids: Journal of Vertebrate Paleontology, v. 4, p. 265–272.

James, G.T., 1963. Paleontology and nonmarine stratigraphy of the Cuyama Valley badlands, California Part 1. Geology, faunal interpretations, and systematic descriptions of Chiroptera, Insectivora, and Rodentia: University of California Publications in Geological Sciences, v. 45, p. 1–154.

Keith, M.S., 2015, Phylogenetic relationships, divergence and radiation within the subfamily Neotominae (Rodentia: Cricetidae) [Ph.D. Dissertation]: Lubbock, Texas Tech University, 166 p.

Kellogg, L., 1910. Rodent fauna of the late Tertiary beds at Virgin Valley and Thousand Creek, Nevada: University of California Publications, Bulletin of the Department of Geology, v. 5, p. 411–437.

Kelly, T.S., 2013, New Hemphillian (late Miocene) rodents from the Coal Valley Formation, Smith Valley, Nevada: Paludicola, v. 9, p. 70–96.

Kelly, T.S., and Whistler, D.P., 2014, New late Miocene (latest Clarendonian to early Hemphillian) cricetid rodents from the upper part of the Dove Spring formation, Mojave Desert, California: Paludicola, v. 10, p. 1–48.

Kelly, T.S., Martin, R.A., and Ronez, C., 2020, New records of cricetid rodents from the medial Clarendonian (middle Miocene) Esmeralda Formation, Fish Lake Valley, Nevada: Paludicola, v. 13, p. 1–32.

Korth, W.W., 2011, New species of cricetid rodents (Mammalia) from the late Miocene (Hemphillian) previously referred to *Peromyscus pliocenicus*: Annals of Carnegie Museum, v. 79, p. 137–147.

Korth, W.W., and De Blieux, D.D., 2010, Rodents and lagomorphs (Mammalia) from the Hemphillian (late Miocene) of Utah: Journal of Vertebrate Paleontology, v. 30, p. 226–235.

León-Tapia, M.A., and Cervantes, F.A., 2021, Systematics and the unexpected high mitochrondrial genetic divergence of *Nelsonia goldmani* (Rodentia: Cricetidae) from Mexican highlands: Journal of Mammalian Evolution, v. 28, p. 939–951.

Lindsay, E.H., 1972, Small mammal fossils from the Barstow Formation, California. University of California Publications in Geological Sciences, v. 93, p. 1–104.

Lindsay, E.H., 2008, Cricetidae, *in* Janis, C.M., Gunnell, G.F., and Uhen M.D., eds., Evolution of Tertiary Mammals of North America: New York, Cambridge University Press, p. 456–479.

Lindsay, E.H., and Jacobs, L.L., 1984, Holarctic radiation of Neogene muroid rodents and the origin of South American cricetids: Journal of Vertebrate Paleontology, v. 4, p. 265–272.

Lindsay, E.H., Mou, Y., Downs, W., Pederson, J., Kelly, T.S., Henry, C., and Trexler, J., 2002, Recognition of the Hemphillian/Blancan boundary in Nevada: Journal of Vertebrate Paleontology, v. 22, p. 429–442.

Martin, J.E., 2008, Hemphillian rodents from northern Oregon and their biostratigraphic implications: Paludicola, v. 6, p. 155–190.

Martin, L.D., 1975, Microtine rodents from the Ogallala Pliocene of Nebraska and the early evolution of the Microtinae in North America., *in* Smith, G.R., and Friedland, N.E., eds., Studies on Cenozoic Paleontology and Stratigraphy in Honor of Claude W. Hibbard: Ann Arbor, Museum of Paleontology, University of Michigan, p. 101–110.

Martin, R.A., and Zakrzewski, R.J., 2019, On the ancestry of woodrats: Journal of Mammalogy, v. 100, p. 1564–1582.

Martin, R.A., Peláez-Campomanes, Honey, J.G., Fox, D.L., Zakrzewski, R.J., Albright, L.B., Lindsay, E.H., Opdyke, N.D., and Goodwin, H.T., 2008, Rodent community change at the Pliocene-Pleistocene transition in southwestern Kansas and identification of the *Microtus* immigration event on the Central Great Plains: Palaeogeography, Palaeoclimatology, Palaeoecology, v. 267, p. 196–207.

Martin, R.A., Peláez-Campomanes, P., Ronez, C., Barbière, F., Kelly, T.S., Lindsay, E.H., and Baskin, J.A., 2020, A new genus of cricetid rodent (Rodentia: Cricetidae) from the Clarendonian (late Miocene) of North America and a consideration of sigmodontine origins: Paludicola, v. 12, p. 298–329.

Matocq, M.D., Shurtliff, Q.R., and Feldman, C.R., 2007, Phylogenetics of the woodrat genus *Neotoma* (Rodentia: Muridae): implications for the evolution of phenotypic variation in male external genitalia: Molecular Phylogenetics and Evolution, v. 42, p. 637–652.

May, S.R., 1981, *Repomys* (Mammalia: Rodentia gen. nov.) from the late Neogene of California and Nevada: Journal of Vertebrate Paleontology, v. 1, p. 218–230.

McClellan, P.H., and Smith, G.R., 2020, Late Miocene fishes of the Cache Valley Member, Salt Lake Formation, Utah and Idaho: Miscellaneous Publications Museum of Zoology, University of Michigan, v. 208, p. 1–54.

Merriam, C.H., 1892a, Description of a new genus and species of murine rodent (*Xenomys nelsoni*) from the state of Colima, western Mexico: Proceedings of the Biological Society of Washington, v. 7, p. 159–163.

Merriam, C.H., 1892b, Descriptions of nine new mammals collected by E. W. Nelson in the states of Colima and Jalisco, Mexico: Proceedings of the Biological Society of Washington, v. 7, p. 164–174.

Merriam, C.H., 1894, A new subfamily of murine rodents—the Neotominae— with description of a new genus and species and a synopsis of the known forms: Proceedings of the Philadelphia Academy of Sciences, v. 46, p. 225–252.

Merriam, C.H., 1897, *Nelsonia neotomodon*, a new genus and species of murine rodent from Mexico: Proceedings of the Biological Society of Washington, v. 11, p. 277–279.

Merriam, C.H., 1898a, Descriptions of twenty new species and a new subgenus of *Peromyscus* from Mexico and Guatemala: Proceedings of the Biological Society of Washington, v. 12, p. 115–125.

Merriam, C.H., 1898b, A new genus (*Neotomodon*) and three new species of murine rodents from the mountains of southern Mexico: Proceedings of the Biological Society of Washington, v. 12, p. 127–129.

Merriam, C.H., 1903, Two new woodrats (genus *Neotoma*) from state of Choahuila, Mexico: Proceedings of the Biological Society of Washington v. 16, p. 47–48.

Miller, J.R., and Engstrom, M.D., 2008, The relationships of major lineages within peromyscine rodents: a molecular phylogenetic hypothesis and systematic reappraisal: Journal of Mammalogy, v. 89, p. 1279–1295.

Mou, Y., 2011, Cricetid rodents from the Pliocene Panaca Formation, southeastern Nevada, USA: Palaeontologia Electronica, v. 14, no. 3, p. 1–53. https://www.uv.es/~pardomv/pe/2011_3/19_mou/index.html.

Musser, G.G., and Carleton, M.D., 2005, Superfamily Muroidea, *in* Wilson, D.E., and Reeder, D.M., eds., Mammal Species of the World, a Taxonomic and Geographic Reference, 3rd Edition: Baltimore, John Hopkins University Press, p. 894–1531.

Ord, G., 1815, North American zoology, *in* Guthrie, W., ed., A New Geographical, Historical and Commercial Grammer; and present state of the several kingdoms of the world: Philadelphia, Johnson and Warner Publishers, v. 2, p. 290–361.

Osgood, W.H., 1909, Revision of the mice of the American genus *Peromyscus*: North American Fauna, v. 28, p. 1–285.

Osgood, W.H., 1938, A new woodrat from Mexico: Field Museum of Natural History, Zoology Series v. 20, p. 475–476.

Reeder, S.A., and Bradley, R.D., 2004, Molecular systematic of Neotomine-peromyscine rodents based on the dentin matrix protein 1 gene: Journal of Mammalogy, v. 85, p. 1194–1200.

Reeder, S.A., Carroll, D.S., Edwards, C.W., Kilpatrick, C.W., and Bradley, R.D., 2006, Neotomine-peromyscine rodent systematics based on combined analysis of nuclear and mitochondrial DNA sequences: Molecular Phylogenetics and Evolution, v. 40, p. 251–258.

Ronez, C., Martin, R.A., and Pardiñas, U.F.J., 2020, Morphological revision of *Copemys loxodon*, type species of the Miocene cricetid *Copemys* (Mammalia, Rodentia): a key to understanding the history of New World cricetids: Journal of Vertebrate Paleontology v. 40, 2. https://doi.org/10.1080/02724634.2020.1772273.

Ronez, C., Martin, R.A., Kelly, T.S., Barbière, F., and Pardiñas, U.F.J., 2021, A brief critical review of sigmodontine rodent origins, with emphasis on paleontological data, *in* Pardiñas, U.F.J., and Galliar, C., eds., Sección Especial El Último Naturalista Tipólogo: Contribuciones en Honor a Elio Massoia, Mendoza, 2021: Mastozoología Neotropical, v. 28, e0495. https://doi.org/10.31687/saremMN.21.28.1.0.07.

Say, T., and Ord, G., 1825, Description of a new species of Mammalia, whereon a new genus is proposed to be found: Journal of the Academy of Natural Sciences, Philadelphia, v. 4, p. 352–355.

Shotwell, J.A., 1967, *Peromyscus* of the late Tertiary in Oregon: Museum of Natural History, University of Oregon, Bulletin 5, p. 1–35.

Silva, M.H., and Cuenca, J.V., 2020a. Molares de la rata cambalachera (*Hodomys alleni elatturus*). http://unibio.unam.mx/irekani/handle/123456789/71598?proyecto=Irekani. [Jan 2021]

Silva, M.H., and Cuenca, J.V., 2020b. Molares de la rata de Magdalena (*Xenomys nelsoni*). http://unibio.unam.mx/irekani/handle/123456789/71607?proyecto=Irekani. [Jan 2021]

Steppan, S.J. and Schenk, J.J., 2017, Muroid rodent phylogenetics: 900-species tree reveals increasing diversification rates: PLoS ONE, v. 12, e0183070. https://doi.org/10.1371/journal.pone.0183070.

Tedford, T.H., Albright III, L.B., Barnosky, A.D., Ferrusquia-Villafranca, I., Hunt, R.M., Jr., Storer, J.E., Swisher, C.C., III, Voorhies, M.R., Webb, S.D., and Whistler, D.P., 2004, Mammalian biochronology of the Arikareean through Hemphillian interval (late Oligocene through early Pliocene epochs), *in* Woodburne, M.O., ed., Late Cretaceous and Cenozoic Mammals of North America: New York, Columbia University Press, p. 169–231.

Thomas, O., 1893, On two new members of the genus *Heteromys* and two of *Neotoma*: Annals and Magazine of Natural History, v. 12, p. 223–235.

Vorontsov, N.N., 1959, [The system of hamsters (Cricetinae) in the sphere of the world fauna and their phylogenetic relations]: Byulleten' Moskovskovo Obshchestva Ispytatelei Prirody, Otdel Biologicheskii, v. 64, p. 134–137. [in Russian]

Wilson, R.W., 1937, New middle Pliocene rodent and lagomorph faunas from Oregon and California: Carnegie Institution of Washington Publication 487, p. 1–19.

Zakrzewski, R.J., 1993, Morphological change in woodrat (Rodentia: Cricetidae) molars, *in* Martin, R.A., and Barnosky, A.D., eds., Morphological Change in Quaternary Mammals of North America: Cambridge, Cambridge University Press, p. 395–407.

Appendix 1. Characters/Character States Used in Cladistic Analyses

1. M1 anteroloph: 0, usually present (>50% of available specimens), long and separated labially from procingulum, originating from junction of procingulum and protoloph 1; 1, short, labially directed, originating from junction of procingulum and protoloph 1 and fused labially with procingulum forming an atoll; 2, absent or vestigial; 3, anteroloph reduced to anterolophule, a short posterolabially directed spur fused to the anterolingual loph at its junction with procingulum in early wear resulting in a narrowing of the paraflexus entrance.
2. M1 parastyle: 0, present; 1, absent.
3. M1 mesoloph/mesolophule: 0, mesoloph present, long, labially directed, isolated from paracone and metacone and originating from hypoloph 1; 1, mesoloph short, labially directed, isolated from paracone and metacone and originating from hypoloph 1; 2, mesoloph significantly reduced to a mesolophule, a short lophule fused anteromedially to paraloph and posterolabially directed; 3, mesoloph significantly reduced, fused anteromedially to paraloph, connecting to metacone in moderate wear; 4, mesoloph/mesolophule absent.
4. M1 mesostyle (not equivalent to the mesostyle of Mou [2011]): 0, usually present (>50%) or present in holotype; 1, absent or usually absent.
5. M1 low cingulum (anterior lingual cingulum, Fig. 1) extending between anterolingual base of protocone to posterolingual base of procingulum, not the

anterolingual cingulum of procingulum): 0, present; 1, absent or vestigial.
6. M1 procingulum bilobed by development of anterolingual conule and well-developed anteromedian flexus: 0, absent or vestigial in very early to early wear; 1, strongly bilobed.
7. M1 protoflexus depth and orientation in occlusal view in early wear: 0, moderately deep, postvergent; 1, shallow, slightly postvergent; 2, usually absent or may be present as slight indentation during early wear.
8. M1 labial flexi in lateral view and labial cingula: 0, V- to U-shaped without shelf-like cingula; 1, U-shaped with well-developed shelf-like cingula.
9. M1 relative position of hypoflexus/paraflexus apices: 0, hypoflexus apex posterior of paraflexus apex; 1, hypoflexus apex nearly opposite of paraflexus apex throughout wear.
10. M1 hypoflexus in lateral view and lingual cingulum: 0, V- to U-shaped without shelf-like cingulum; 1, U-shaped with well-developed shelf-like lingual cingulum.
11. M2 mesoloph/mesolophule: 0, mesoloph long, labially directed, isolated from paracone and metacone and originating from hypoloph 1; 1, mesoloph short, labially directed, isolated from paracone and metacone and originating from hypoloph 1; 2, mesoloph significantly reduced to a mesolophule, a short lophule fused anteromedially to paraloph and posterolabially directed; 3, mesoloph significantly reduced, fused anteromedially to paraloph, connecting to metacone in moderate wear; 4, mesoloph/mesolophule absent.
12. M3 occlusal outline pattern with wear: 0, round to oval; 1, E-shaped; 2, F-shaped.
13. M3 protoflexus: 0, moderately developed; 1, shallow; 2, absent.
14. M3 hypoflexus: 0, moderately to well developed; 1, weakly developed, shallow; 2, absent to vestigial.
15. M3 hypocone: 0, moderately developed; 1, well developed; 2, weakly developed.
16. M3 relative size of talon to trigon (ratio of talon tr/trigon tr), talon includes hypocone, metacone, mesoloph (if present), posteroloph and their connecting lophs, trigon includes anterior cingula (if present), paracone, protocone and their connecting lophs: 0, moderately smaller (0.65-0.75); 1, slightly smaller (≥0.80); 2, significantly smaller (≤0.50).
17. m1 crown height (ratio of m1 protoconid ht/m1 ap when unworn to very early wear): 0, brachydont (<0.50); 1, mesodont to hypsodont due to coronal increase in height (≥0.50).
18. m1 mesolophid (not equal to mesolophid of Zakrzewski, 1993)/mesolophule: 0, mesolophid long, lingually directed and originating from protolophid 2; 1, mesolophid short, anterolingually directed and

originating from protolophid 2; 3, mesolophid significantly reduced to mesolophulid, a short, anterolingually directed projection fused anteromedially to entolophid at initial through early moderate wear; 4, mesolophid/mesolophulid absent.

19. m1 ectolophulid (short, anterolabially directed projection originating from the hypolophid 2 on the occlusal plane: 0, absent; 1, present in very early or early wear.

20. m1 anterior lateral dentine tract: 0, absent; 1, present.

21. m1 procingulid bilobed with addition of second conulid (anterolabial conulid): 0, absent; 1, vestigial to very slightly in very early wear; 2, present through moderate wear; 3, present throughout wear.

22. m1 relative position of procingulid in occlusal view to long axis of tooth: 0, slightly lingually; 1, centrally; 2, slightly labially to labially.

23. m1 protoflexid depth and orientation in occlusal view: 0, moderately deep to deep, provergent; 1, extremely deep, constricted near termination forming incipient atoll, provergent; 2, moderately deep and nearly perpendicular to long axis of tooth.

24. m1 entoflexid depth and orientation in occlusal view (or mesoflexid when well-developed, long mesolophid present dividing the reentrant): 0, very deep, provergent; 1, very deep and slightly provergent to nearly perpendicular to long axis of tooth.

25. m1 labial flexids in lateral view and labial cingulid: 0, V- to U- shaped without shelf-like cingulids; 1, U-shaped with well-developed shelf-like labial cingulids.

26. m1 metaflexid relative positions of metaconid/procingulid and atoll: 0, moderately deep, U-shaped, metaconid separated from procingulid until very late wear; 1, moderately deep, metaconid and procingulid lingual margins closely positioned, fusing in early to early moderate wear forming an atoll; 2, moderately deep, metaconid and procingulid closely positioned, but separate through moderate wear, fusing during very late wear; 3, shallow, metaconid and procingulid connected in initial to very early wear, atoll present near anterolabial margin of metaflexid; 4, shallow, metaconid and procingulid connected in initial wear, atoll sometimes present in center of procingulid; 5, deep, wide V-shaped with metaconid and procingulid well separated through very late wear; 6, usually absent, but sometimes present as small transient notch.

27. m1 hypoflexid in lateral view and labial cingulid: 0, V- to U-shaped without well-developed shelf-like cingulid; 1, U-shaped with well-developed shelf-like labial cingulid.

28. m1 posteroflexid depth and orientation in occlusal view: 0, deep, provergent; 1, deep, slightly provergent to nearly perpendicular to long axis of tooth.

29. m1 hypoflexid/posteroflexid relative positions of apices in occlusal view: 0, hypoflexid apex anterior of posteroflexid apex; 1, hypoflexid apex opposite to posteroflexid apex.

30. m1 procingulid anterolabial cingulid/protoflexid pocket (also applies to m2). Pocket is defined as deep protoflexid completely enclosed labially by a tall anterolabial cingulid that forms a pocket-like appearance in occlusal view (Fig. 2.6); 0, moderately to well developed, extending posteriorly and connected to base of protoconid, protoflexid not pocketed; 1, moderately to well developed not extending to base of protoconid, protoflexid not pocketed; 2, cingulid well developed, extending posteriorly and connected to base of protoconid, protoflexid strongly pocketed; 3, cingulid weakly developed, widely separated from protoconid, protoflexid not pocketed.

31. m2 ectolophulid (short, anterolabially directed projection originating from hypolophid 1 on occlusal plane): 0, absent; 1, present in very early or early wear.

32. m3 occlusal outline pattern: 0, S-shaped; 1, oblique keyhole-shaped (talonid flexed lingually); 2, keyhole-shaped; 3, dumbbell-shaped (bilobed).

33. m3 mesolophid (not equal to mesolophid of Zakrzewski [1993]): 0, present, long; 1, present, short; 2, absent.

34. m3 entoflexid (or mesoflexid if well-developed mesolophid present in reentrant)/atoll: 0, moderately deep, open lingually, does not close with wear, no atoll; 1, deep, initially open lingually and then closes off by early moderate to moderate wear forming an atoll; 2, shallow, entoflexid closed at initial wear with atoll present between metaconid and protoconid; 3, entoflexid very deep, straight, widely open lingually throughout wear, no atoll.

35. m3 entoflexid/hypoflexid apices: 0, entoflexid apex anterior to hypoflexid apex; 1, entoflexid apex opposite of hypoflexid apex.

36. m3 posteroflexid: 0, present; 1, absent.

37. m3 talonid size relative to trigonid size (talonid tr/trigonid tr ratio), talon includes hypoconid, entoconid, mesolophid (if present), posterolophid and their connecting lophids), trigon includes anterior cingulids (if present), metaconid, protoconid and their connecting lophids: 0, moderately smaller (0.65–0.75); 1, slightly smaller (≥0.80); 2, significantly smaller (≤0.55).

38. Dentary, mental foramen relative size and position on horizontal ramus: 0, large size, lateral and moderately high; 1, moderate size, lateral and moderately high; 2, moderate size, lateral and very high; 3, small size, lateral and moderately high.

39. Dentary, position of masseteric scar on horizontal ramus: 0, about the middle; 1, low.

40. Dentary, development of incisor capsular process: 0, well developed; 1, weakly developed.

Appendix 2. Character state matrix for analysis with the following species: *Copemys loxodon, Protorepomys bartlettensis, P. mckayensis, Tsaphanomys shotwelli, Paronychomys jacobsi, P. lemredfieldi, Miotomodon mayi, Basirepomys pliocenicus, B. romensis, B. robertsi, Galushamys redingtonensis, Repomys gustelyi, Lindsaymys takeuchii, Neotoma (Paraneotoma) quadriplicata, Neotoma cinerea, Neotoma lepida, Hodomys alleni, Nelsonia goldmani, and Xenomys nelsoni.*

Character numbers

Taxon	1	2	3	4	5	6	7	8	9	10	11	12	13	14	15	16	17	18	19	20
C. loxodon	0	0	0	0	0	0	0	0	0	0	0	0	0	0	0	0	0	0	0	0
P. bartlettensis	1	1	1	1	1	0	0	0	0	0	?	0	0	0	0	0	1	1	0	0
P. mckayensis	2	1	4	1	1	0	0	0	0	0	2	?	?	?	?	?	1	3	0	0
T. shotwelli	2	1	4	1	1	0	0	0	0	0	4	?	?	?	?	?	1	4	0	0
P. jacobsi	2	1	4	1	1	0	0	1	0	1	4	0	1	2	3	0	1	4	0	0
P. lemredfieldi	2	1	4	1	1	0	0	1	0	1	4	0	1	2	3	0	1	4	0	0
M. mayi	3	1	2	1	1	0	0	0	0	0	2	0	0	0	0	1	1	?	0	0
B. pliocenicus	2	1	4	1	0	0	0	?	0	?	4	?	?	?	?	?	1	4	0	0
B. romensis	2	0	0	0	0	1	0	0	0	0	1	?	?	?	?	?	1	0	0	0
B. robertsi	2	1	0	0	0	0	0	0	0	?	1	?	?	?	?	?	1	4	0	0
G. redingtonensis	2	1	3	1	1	0	1	?	0	?	3	0	1	1	2	2	?	?	?	0
R. gustelyi	3	1	2	1	1	0	0	0	0	0	2	2	1	1	2	2	1	3	1	0
L. takeuchii	2	1	4	1	1	0	0	0	0	0	4	0	2	0	0	1	1	4	0	0
N. quadriplicata	2	1	4	1	1	0	0	0	0	0	4	1	2	0	1	1	1	4	0	0
N. cinerea	2	1	4	1	1	0	0	0	1	0	4	1	2	0	1	1	1	4	0	1
N. lepida	2	1	4	1	1	0	2	0	1	0	4	1	2	0	1	1	1	4	0	0
H. alleni	2	1	4	1	1	0	0	0	0	0	4	1	2	0	1	1	1	4	0	0
N. goldmani	3	1	2	1	1	0	0	0	0	0	2	2	2	1	2	2	1	3	1	0
X. nelsoni	2	1	4	1	1	0	0	0	0	0	4	1	2	0	1	1	1	4	0	0

Character numbers

Taxon	21	22	23	24	25	26	27	28	29	30	31	32	33	34	35	36	37	38	39	40
C. loxodon	0	0	0	0	0	0	0	0	0	0	0	0	0	0	0	0	0	0	0	0
P. bartlettensis	0	1	1	0	0	1	0	0	0	1	?	0	2	1	0	0	0	?	?	?
P. mckayensis	0	1	0	0	0	4	0	0	0	1	0	0	2	1	0	1	0	?	?	?
T. shotwelli	0	1	0	0	0	3	0	0	0	1	0	0	2	1	0	1	0	?	?	?
P. jacobsi	0	1	0	0	1	1	1	0	0	2	0	0	2	0	0	0	0	0	0	0
P. lemredfieldi	1	1	0	0	1	1	1	0	0	2	0	0	2	0	0	0	0	0	0	0
M. mayi	0	1	0	0	0	3	0	0	0	1	0	?	?	?	0	?	0	1	0	0
B. pliocenicus	2	1	0	0	0	2	0	0	0	1	0	?	?	?	0	?	?	0	0	?
B. romensis	1	1	0	0	0	2	0	0	0	1	0	0	1	0	0	0	0	0	0	0
B. robertsi	3	1	0	0	?	2	2	0	0	1	0	0	1	0	0	0	0	0	0	0
G. redingtonensis	0	1	0	0	?	?	?	?	0	?	?	?	?	?	0	?	?	?	?	?
R. gustelyi	0	1	0	0	0	4	0	0	0	1	1	2	2	2	0	1	2	1	0	?
L. takeuchii	0	1	0	0	0	1	0	0	0	1	0	0	2	1	0	1	0	?	?	?
N. quadriplicata	0	1	0	0	0	3	0	1	0	1	0	0	2	1	0	1	1	2	0	0
N. cinerea	0	2	2	1	0	5	0	1	1	3	0	3	2	3	1	1	1	2	0	0
N. lepida	0	2	2	1	0	6	0	1	1	3	0	3	2	3	1	1	1	2	0	0
H. alleni	0	2	2	1	0	5	0	1	0	3	0	0	2	3	0	1	1	3	1	1
N. goldmani	0	1	0	0	0	4	0	0	0	1	1	1	2	2	0	1	2	1	0	1
X. nelsoni	0	2	2	1	0	5	0	1	0	3	0	0	2	3	0	1	1	3	1	1